

Gluon saturation effects on the color singlet J/ψ production in high energy dA and AA collisions

F. Dominguez,¹ D.E. Kharzeev,^{2,3} E.M. Levin,^{4,5} A.H. Mueller,¹ and K. Tuchin⁶

¹*Department of Physics, Columbia University, New York, NY 10027, USA*

²*Department of Physics and Astronomy, Stony Brook University, Stony Brook, NY 11794, USA*

³*Department of Physics, Brookhaven National Laboratory, Upton, NY 11973-5000, USA*

⁴*HEP Department, School of Physics, Raymond and Beverly Sackler Faculty of Exact Science,
Tel Aviv University, Tel Aviv 69978, Israel*

⁵*Departamento de Física, Universidad Técnica Federico Santa María,
Avda. España 1680, Casilla 110-V, Valparaíso, Chile*

⁶*Department of Physics and Astronomy, Iowa State University, Ames, IA 50011, USA*

(Dated: February 18, 2022)

We derive the formulae for the cross section of J/ψ production in high energy pA and AA collisions taking into account the gluon saturation/color glass condensate effects. We then perform the numerical calculations of the corresponding nuclear modification factors and find a good agreement between our calculations and the experimental data on J/ψ production in pA collisions. We also observe that cold nuclear modification effects alone cannot describe the data on J/ψ production in AA collisions. Additional final state suppression (at RHIC) and enhancement (at LHC) mechanisms are required to explain the experimental observations.

I. INTRODUCTION

The goal of this paper is to provide an improved analysis of the gluon saturation effects on the color singlet mechanism of J/ψ production in dA and AA collisions at RHIC and LHC. In our recent publications [1–3] we argued that a mechanism responsible for J/ψ production in central nuclear collisions is different from the one in pp collisions. This is because the symmetry properties of J/ψ under the parity and charge conjugation transformations dictate that there must be an odd number of gluons attached to the bound c and \bar{c} quarks. At the lowest order in strong coupling α_s there are three gluons attached. In pp collisions, two of those gluons have their external ends attached to the valence quarks of the colliding protons whereas the third one is emitted by the $c\bar{c}$ dipole. On the other hand in central pA collisions the parametrically enhanced contribution in the quasi-classical regime – which is controlled by a large parameter $\alpha_s^2 A^{1/3} \sim 1$ [4–6] – originates from the diagrams where one of the gluons is attached to the proton’s valence quark whereas the remaining two are attached to the valence quarks inside two different nucleons of the nucleus.

Obviously, such contribution breaks the perturbative QCD factorization already at the leading order in α_s .

In [1] we assumed that the $c\bar{c}$ pair propagates through the nucleus in the color octet state and becomes color singlet only after the last interaction with the nucleus. In this paper we drop this assumption by taking into account a possibility that the $c\bar{c}$ pair converts from the color octet to the color singlet state already inside the nucleus. In the large N_c approximation further color conversions of the $c\bar{c}$ state are suppressed and thus can be neglected. Therefore, in this case the $c\bar{c}$ experiences the last inelastic interaction inside the nucleus after which it rescatters only elastically. As a result, the last inelastic interaction does not exponentiate with the rest of the scatterings and – as we will show – automatically selects an odd number of inelastic scatterings as required by the parity of J/ψ . This is different from our approach in [1–3] where we had to select the odd number of inelastic scatterings in the scattering amplitude. Additionally, we give a more accurate treatment of J/ψ wave function with parameters taken from a fit to the exclusive J/ψ production in deep inelastic scattering.

Our paper is structured as follows. In Sec. II we derive the cross section for J/ψ production in pA collisions; our main result is given by Eq. (15). In Sec. III we propose a generalization of this result to the AA collisions. The derived cross section is given by (17),(18) and satisfies the constraints imposed by the symmetry of the J/ψ wave function. The results in Sec. II and Sec. III are derived in the quasi-classical approximation, i.e. assuming that the coherence length for J/ψ production is much larger than the nuclear radius, but neglecting the low- x evolution. In Sec. IV we derive expression for the scattering amplitude (26) that includes the low- x evolution and thus gives a dependence on energy and rapidity. Sec. V is dedicated to the description of the numerical calculations performed with different models for the dipole scattering amplitudes. Our main results are exhibited in Figs. 3,4. We discuss them and conclude in Sec. VI.

II. PRODUCTION OF J/ψ IN PA COLLISIONS

The cross section for J/ψ production in pA collisions can be written in the factorized form

$$\frac{d\sigma_{pA \rightarrow J/\psi X}}{d^2b dy} = x_1 G(x_1, m_c^2) \frac{d\sigma_{gA \rightarrow J/\psi X}}{d^2b}. \quad (1)$$

In order to set normalizations for $\frac{d\sigma_{gA \rightarrow J/\psi X}}{d^2b}$ it is convenient to compare the gA scattering process in (1) with that of γA where there is a well developed phenomenology. Start with γ -proton scattering

where

$$\frac{d\sigma_{\gamma p \rightarrow J/\psi p}}{dt} = \frac{1}{16\pi} |A_{\gamma p \rightarrow J/\psi p}|^2 \quad (2)$$

with

$$A_{\gamma p \rightarrow J/\psi p}(x, \Delta) = \int d^2b e^{-i\Delta \cdot b} \int_0^1 dz \int \frac{d^2r}{4\pi} \left(\psi_{J/\psi}^* \psi_\gamma \right) 2i [1 - S(x, \mathbf{r}, \mathbf{b})] \quad (3)$$

and t is given in terms of the momentum transfer by $t = -\Delta^2$. Call

$$\left(\psi_{J/\psi}^* \psi_\gamma \right) = \Phi_\gamma(\mathbf{r}, z) \quad (4)$$

where

$$\Phi_\gamma(\mathbf{r}, z) = \frac{2}{3} e \frac{N_c}{\pi} \left\{ m_c^2 K_0(m_c r) \phi_T(r, z) - [z^2 + (1-z)^2] m_c K_1(m_c r) \partial_r \phi_T(r, z) \right\} \quad (5)$$

with [7, 8]

$$\phi_T(r, z) = N_T z(1-z) \exp \left[-\frac{r^2}{2R_T^2} \right] \quad (6)$$

and where $N_T = 1.23$, $R_T^2 = 6.5 \text{ GeV}^{-2}$ [8].

Except for a factor of $z(1-z)$ in (6) our notation, and choice of J/ψ wave function exactly matches that of Ref. [9]. Because (1) is a collinear factorized expression the gluon projectile on the right hand side of (1) is on-shell and so only transverse polarizations appear. We have taken the photon in (2) also on-shell so that the relationship between the photon and gluon induced processes will involve only a normalization change in (5) and a change of the $1 - S$ factor in (3).

We can get (2) in a more convenient form by using (3) and integrating over Δ . Thus

$$\frac{d\sigma_{\gamma A \rightarrow J/\psi A'}}{d^2b} = \int_0^1 dz \int \frac{d^2r}{4\pi} \Phi_\gamma(\mathbf{r}, z) \int_0^1 dz' \int \frac{d^2r'}{4\pi} \Phi_\gamma^*(\mathbf{r}', z') [1 - S^*(r')] [1 - S(r)] \quad (7)$$

where we have suppressed the energy and impact parameter dependence in the $1 - S$ factors in (7). The S factors are given, in the McLerran-Venugopalan model [4], by

$$S(r) = \exp \left[-\frac{C_F}{N_c} \frac{Q_s^2}{4} r^2 \right] \simeq \exp \left[-\frac{1}{8} Q_s^2 r^2 \right] \quad (8)$$

and the cross section in (7) allows nuclear breakup but is elastic at the dipole-nucleon scattering level. Q_s in (8) is the gluon saturation momentum with impact parameter dependence again suppressed.

The main change necessary to convert (7) to a cross section for $gA \rightarrow J/\psi X$ is the way the $c\bar{c}$ dipole scatters off nucleons in the nucleus. In (7) the scatterings are purely elastic, and such

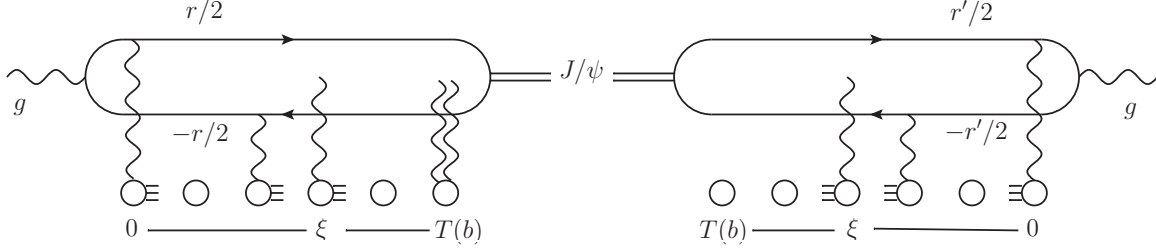


FIG. 1: Sample diagram contributing to the $gA \rightarrow J/\psi$ process. The point of the last inelastic interaction is signaled explicitly at the longitudinal coordinate ξ .

scatterings are dominant in the large- N_c limit because the quantum numbers of the γ and the J/ψ are the same. In gA collisions the $c\bar{c}$ pair emerging from the gluon is in the adjoint color representation. The $c\bar{c}$ forming the J/ψ is, of course, a color singlet. In the large- N_c approximation there is a particular dipole-nucleon inelastic collision which converts the adjoint representation to a color singlet. This inelastic interaction is at the longitudinal coordinate ξ , starting from the front of the nucleus, in Fig. 1. Later interactions, occurring after the $c\bar{c}$ pair is in a singlet state, are purely elastic in order to keep the singlet intact. Earlier interactions, occurring while the $c\bar{c}$ is in the adjoint representation, may be either elastic, occurring off a *single* c or \bar{c} in the amplitude or complex conjugate amplitude, or inelastic involving the c in both the amplitude and complex conjugate amplitude or involving the \bar{c} in both the amplitude and complex conjugate amplitude. Sample interactions are illustrated in Fig. 1.

The interaction at ξ gives the factor

$$\frac{Q_s^2 \mathbf{r} \cdot \mathbf{r}'}{4T(b)} d\xi. \quad (9)$$

The interactions occurring before ξ give the factor

$$e^{-\frac{1}{16}Q_s^2(\mathbf{r}-\mathbf{r}')^2(\xi/T(b))} \quad (10)$$

while those occurring after give

$$e^{-\frac{1}{8}Q_s^2(r^2+r'^2)(1-\xi/T(b))}. \quad (11)$$

In going from $\gamma A \rightarrow J/\psi A'$ to $gA \rightarrow J/\psi X$ the $[1 - S^*(r')][1 - S(r)]$ factor in (7) gets replaced by the product of the factors in (9)-(11).

In addition there is a color factor. In γ induced J/ψ production there is a factor of N_c in the amplitude and a factor of N_c in the complex conjugate amplitude. This is the factor of N_c explicit

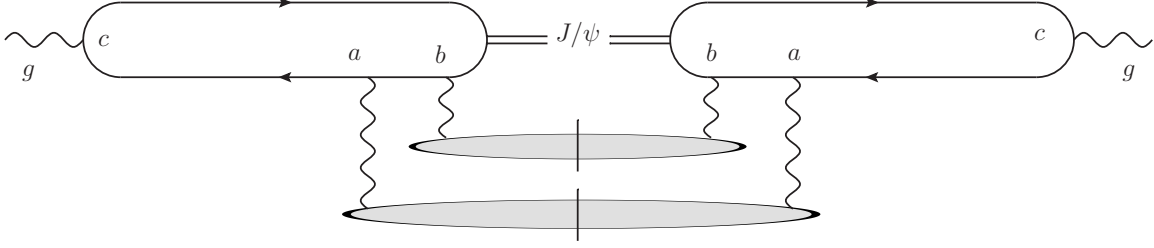


FIG. 2: Lowest order process in gluon induced J/ψ production. Color indices are indicated explicitly.

in (5) coming from a sum over the colors of the c , and \bar{c} , making up the J/ψ . To find the color factors in the gluon induced process it is necessary to evaluate the lowest order process shown in Fig. 2. The color factors for this process are, as already found in [2],

$$\frac{1}{(N_c^2 - 1)^3} \text{Tr} \left(t^c t^a t^b \right) \text{Tr} \left(t^c t^b t^a \right) \simeq \left(\frac{C_F}{N_c^2 - 1} \right)^2 \frac{1}{2N_c} \quad (12)$$

where we have used the large- N_c limit in the right hand side of (12). The $(C_F/(N_c^2 - 1))^2$ factors go into making up part of the two factors of Q_s^2 that come from the graphs. Explicit calculation confirms that the remaining factor, after taking out the factor in (9) and the factor linear in Q_s^2 when expanding (10) is just the factor $1/2N_c$ on the right hand side of (12).

Putting all this together gives

$$\begin{aligned} \frac{d\sigma_{gA \rightarrow J/\psi X}}{d^2b} &= \int_0^1 dz \int \frac{d^2r}{4\pi} \Phi(\mathbf{r}, z) \int_0^1 dz' \int \frac{d^2r'}{4\pi} \Phi^*(\mathbf{r}', z') \\ &\times \int_0^{T(b)} d\xi \frac{\mathbf{r} \cdot \mathbf{r}' Q_s^2}{4T(b)} \exp \left\{ -\frac{1}{16} Q_s^2 (\mathbf{r} - \mathbf{r}')^2 \frac{\xi}{T(b)} - \frac{1}{8} Q_s^2 (r^2 + r'^2) \left(1 - \frac{\xi}{T(b)} \right) \right\} \end{aligned} \quad (13)$$

with

$$\Phi(\mathbf{r}, z) = \left[\frac{2}{3} e N_c \right]^{-1} \frac{g}{\sqrt{2N_c}} \Phi_\gamma(\mathbf{r}, z) \quad (14)$$

where, finally, in (14) we have introduced the replacement $\frac{2}{3}e \rightarrow g$. Doing the integral over ξ and using (1) we get

$$\begin{aligned} \frac{d\sigma_{pA \rightarrow J/\psi X}}{dy d^2b} &= x_1 G(x_1, m_c^2) \int_0^1 dz \int \frac{d^2r}{4\pi} \Phi(\mathbf{r}, z) \int_0^1 dz' \int \frac{d^2r'}{4\pi} \Phi^*(\mathbf{r}', z') \\ &\times \frac{4\mathbf{r} \cdot \mathbf{r}'}{(\mathbf{r} + \mathbf{r}')^2} \left(e^{-\frac{Q_s^2}{16} (\mathbf{r} - \mathbf{r}')^2} - e^{-\frac{Q_s^2}{8} (r^2 + r'^2)} \right). \end{aligned} \quad (15)$$

III. J/ψ CROSS SECTION IN AA COLLISIONS

Generalization of the result of the previous section to nucleus-nucleus collisions is achieved by letting the initial gluon be emitted from either nucleus and taking into account $c\bar{c}$ dipole scattering in both nuclei. The scattering amplitudes and the saturation scales for the two nuclei depend on their respective impact parameters \mathbf{b}_1 and \mathbf{b}_2 . To make our notations more compact we will not indicate the impact parameter dependence explicitly. Introducing the relative impact parameter $\mathbf{B} = \mathbf{b}_1 - \mathbf{b}_2$ and using the relation

$$\frac{\alpha_s \pi^2}{4C_F} x_1 G(x_1, a^2) = \int d^2 b_1 \frac{Q_{s1}^2}{8} \quad (16)$$

we can write the cross section as

$$\frac{d\sigma_{A_1 A_2 \rightarrow J/\psi X}}{dy d^2 b d^2 B} = \int_0^1 dz \int \frac{d^2 \mathbf{r}}{4\pi} \int_0^1 dz' \int \frac{d^2 \mathbf{r}'}{4\pi} \Phi(\mathbf{r}, z) \Phi_{\lambda\lambda'}^*(\mathbf{r}', z') 2T_{A_1 A_2 \rightarrow JX}(\mathbf{r}, \mathbf{r}'), \quad (17)$$

where

$$T_{A_1 A_2 \rightarrow JX}(\mathbf{r}, \mathbf{r}') = \frac{C_F}{2\alpha_s \pi^2} \frac{Q_{s1}^2 Q_{s2}^2}{Q_{s1}^2 + Q_{s2}^2} \frac{4\mathbf{r} \cdot \mathbf{r}'}{(\mathbf{r} + \mathbf{r}')^2} \left(e^{-\frac{1}{16}(Q_{s1}^2 + Q_{s2}^2)(\mathbf{r} - \mathbf{r}')^2} - e^{-\frac{1}{8}(Q_{s1}^2 + Q_{s2}^2)(r^2 + r'^2)} \right) \quad (18)$$

Expanding (18) at small Q_{s1}^2 we recover Eq. (15).

The first few terms in the expansion of (18) in nuclear density read

$$T_{A_1 A_2 \rightarrow JX}(\mathbf{r}, \mathbf{r}') \approx \frac{C_F}{2\alpha_s \pi^2} Q_{s1}^2 Q_{s2}^2 4\mathbf{r} \cdot \mathbf{r}' \left(\frac{1}{16} - \frac{1}{512} (Q_{s1}^2 + Q_{s2}^2) (3r^2 + 3r'^2 - 2\mathbf{r} \cdot \mathbf{r}') \right) \quad (19)$$

Averaging over the relative angle between \mathbf{r} and \mathbf{r}' yields

$$\langle T_{A_1 A_2 \rightarrow JX}(\mathbf{r}, \mathbf{r}') \rangle \approx \frac{C_F}{\alpha_s \pi^2} \frac{r^2 r'^2}{16^2} (Q_{s1}^2 Q_{s2}^4 + Q_{s1}^4 Q_{s2}^2) \quad (20)$$

This is the leading contribution to the J/ψ production; it is easily seen that it breaks the factorization. We believe that (18) is a reasonable starting point for phenomenology of J/ψ production in AA collisions. Nevertheless a better theoretical understanding of the AA production amplitude $T_{A_1 A_2 \rightarrow J/\psi X}$ is desirable.

IV. RAPIDITY AND ENERGY DEPENDENCE

Eqs. (17),(18) can be readily generalized to include quantum evolution effects. To that end we recall that the initial condition for the BK [5, 10] evolution equation is given by the Glauber–Mueller formula for the forward dipole–nucleus quark dipole elastic scattering amplitude [11]

$$N_F(\mathbf{r}, \mathbf{b}, y_0) = 1 - e^{-\frac{1}{8}\mathbf{r}^2 Q_s^2(y_0)}, \quad (21)$$

where subscript F indicates the fundamental representation. Evolution of the gluon dipole scattering amplitude (adjoint representation) obeys the equation

$$N_A(\mathbf{r}, \mathbf{b}, y) = 2N_F(\mathbf{r}, \mathbf{b}, y) - N_F^2(\mathbf{r}, \mathbf{b}, y) \quad (22)$$

and its initial condition is

$$N_A(\mathbf{r}, \mathbf{b}, y_0) = 1 - e^{-\frac{1}{4}\mathbf{r}^2 Q_s^2(y_0)}, \quad (23)$$

Accordingly, we can incorporate evolution effects in (18) by the following replacements [12]

$$e^{-\frac{1}{8}Q_s^2 r^2} \rightarrow 1 - N_F(\mathbf{r}, \mathbf{b}, y) \quad (24)$$

$$e^{-\frac{1}{16}Q_s^2 r^2} \rightarrow 1 - N_A(\mathbf{r}/2, \mathbf{b}, y) \quad (25)$$

Omitting the impact parameter dependence as before, we thus obtain

$$\begin{aligned} T_{A_1 A_2 \rightarrow JX}(\mathbf{r}, \mathbf{r}') = & \frac{8N_c}{\alpha_s \pi^2} \frac{Q_{s1}^2 Q_{s2}^2}{Q_{s1}^2 + Q_{s2}^2} \frac{4\mathbf{r} \cdot \mathbf{r}'}{(\mathbf{r} + \mathbf{r}')^2} \left\{ \left[1 - N_A^{(1)}((\mathbf{r} - \mathbf{r}')/2, y) \right] \left[1 - N_A^{(2)}((\mathbf{r} - \mathbf{r}')/2, -y) \right] \right. \\ & \left. - \left[1 - N_F^{(1)}(\mathbf{r}, y) \right] \left[1 - N_F^{(1)}(\mathbf{r}', y) \right] \left[1 - N_F^{(2)}(\mathbf{r}, -y) \right] \left[1 - N_F^{(2)}(\mathbf{r}', -y) \right] \right\} \end{aligned} \quad (26)$$

V. NUMERICAL CALCULATIONS

The experimental data is expressed in terms of the nuclear modification factor (NMF) defined as

$$R_{A_1 A_2} = \frac{\int_{\mathcal{S}} d^2b \frac{d\sigma_{A_1 A_2 \rightarrow J/\psi X}}{dy d^2b}}{A_1 A_2 \frac{d\sigma_{pp \rightarrow J/\psi X}}{dy}}. \quad (27)$$

where \mathcal{S} stands for the overall area of two colliding nuclei. Since the mechanism of J/ψ production in pp collisions remains elusive, we follow our approach in the previous publications and approximate

$$\frac{d\sigma_{pp \rightarrow J/\psi X}}{dy} = C \frac{d\sigma_{AA \rightarrow J/\psi X}}{dy} \Big|_{A=1} \quad (28)$$

with $C = \text{const.}$ We fix the constant to provide the best description of the pp and dA data. It is reassuring that the numerical calculations described in the next section indicate that C is close to unity.

The results of our calculations are exhibited in Fig. 3 and Fig. 4; we have used two different models for the dipole scattering amplitude: DHJ [13] and bCGC [9] models (see Appendix A for the description of these models). Comparison of the results of the two models gives an idea

about the model dependence of the numerical results. We observe a reasonable agreement with the experimental data on J/ψ production in dA collisions.

Concerning the J/ψ production in AA collisions all models underestimate the suppression at RHIC both at mid-rapidity and in the forward rapidity. Moreover, it appears that the gluon saturation effects on NMF show very little rapidity dependence at RHIC which contradicts the experimental data. We also find that there is almost no change between the NMF at LHC $\sqrt{s} = 2.76$ TeV and 5.5 TeV. We note that our calculation overestimates the NMF at $\sqrt{s} = 2.76$ TeV.

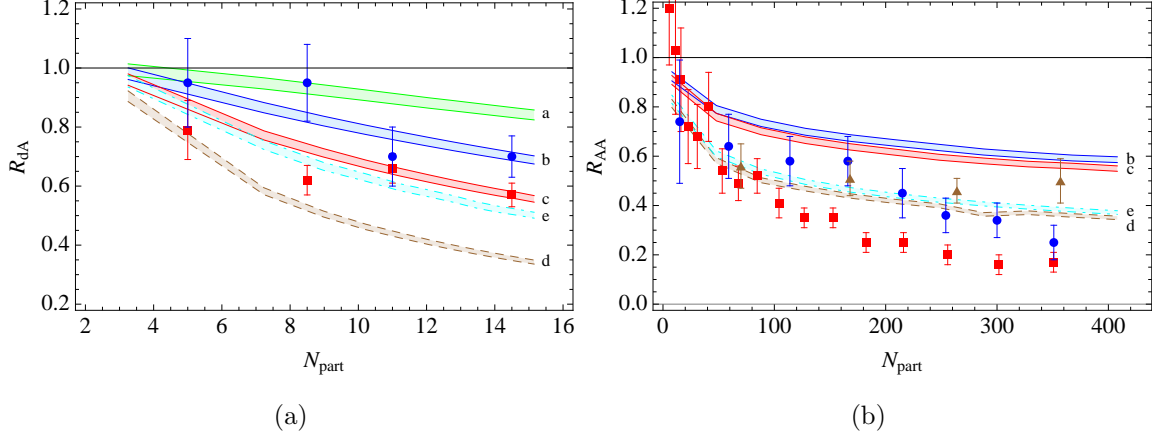


FIG. 3: Nuclear modification factor vs N_{part} in (a) dAu and (b) AA collisions using the DHJ model [13]. Band ‘a’ (green) represents rapidity $y = -1.7$ at $\sqrt{s} = 200$ GeV, ‘b’ (blue): $y = 0$, $\sqrt{s} = 200$ GeV, ‘c’ (red): $y = 1.7$, $\sqrt{s} = 200$ GeV, ‘d’ (brown): $y = 3.25$, $\sqrt{s} = 2.76$ TeV, ‘e’ (cyan): $y = 0$, $\sqrt{s} = 5.5$ TeV. $m = 1.5$ GeV, $C = 1$. Experimental data [16–19] is represented by (blue) circles in ‘b’, by (red) squares in ‘c’ and by (brown) triangles in ‘d’. (Color online).

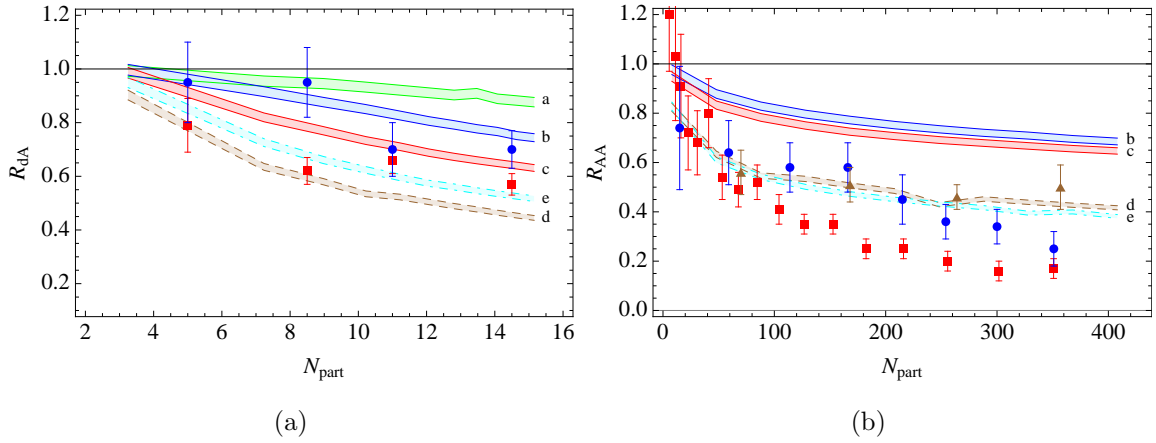


FIG. 4: Same as Fig. 3 using the bCGC model [9].

VI. DISCUSSION AND CONCLUSIONS

Our calculations indicate that the nuclear modification of J/ψ production in dA collisions at RHIC is dominated by the cold nuclear matter effects. It would be important to study J/ψ production in pA collisions at LHC; Fig. 3 and Fig. 4 provide our predictions. In contrast, the cold nuclear matter effects alone cannot provide neither quantitative nor even a qualitative description of the AA data. Additional mechanisms beyond the initial state effects are required to explain the experimental data. It is remarkable that at RHIC these additional mechanisms must provide extra suppression of the NMF, perhaps via the Matsui-Satz color screening mechanism [20] or the gluon-induced dissociation [24, 25], whereas at LHC they must produce enhancement.

Our successful description of the J/ψ NMF in pA collisions with the normalization factor $C = 1$ in (28) may be an evidence that the J/ψ production mechanism in pp collisions is similar to that in pA implying that it is perhaps dominated by the higher twist effects.

To summarize, we derived the formulae for the cross sections of J/ψ production in pA and AA collisions taking into account the gluon saturation/color glass condensate effects. Our numerical results provide an estimate of the color nuclear matter effects on J/ψ production in heavy-ion collisions.

Acknowledgments

The work of D.K. was supported in part by the U.S. Department of Energy under Contracts No. DE-AC02-98CH10886 and DE-FG-88ER41723. K.T. was supported in part by the U.S. Department of Energy under Grant No. DE-FG02-87ER40371. This research of E.L. was supported in part by the Fondecyt (Chile) grant 1100648.

Appendix A: Models of the dipole scattering amplitude

We performed numerical calculations using two models of the dipole scattering amplitude: DHJ [13] and bCGC [9] models. The DHJ model is an improvement of the KKT model[14, 21] that takes into account the change in the anomalous dimension of the gluon distribution function due to the presence of the saturation boundary [15] and takes into account some higher order effect. It successfully describes the single inclusive hadron production in dA collisions in the relevant

kinematic region. In this model, the dipole scattering amplitude is parameterized as follows

$$N_A(\mathbf{r}, 0, y) = 1 - \exp \left\{ -\frac{1}{4} (r^2 Q_s^2)^\gamma \right\}. \quad (\text{A1})$$

The *gluon* saturation scale is given by

$$Q_s^2 = \Lambda^2 A^{1/3} e^{\lambda y} = 0.13 \text{ GeV}^2 e^{\lambda y} N_{\text{coll}}. \quad (\text{A2})$$

where the parameters $\Lambda = 0.6 \text{ GeV}$ and $\lambda = 0.3$ are fixed by DIS data [22].

$$\gamma = \gamma_s + (1 - \gamma_s) \frac{\ln(m^2/Q_s^2)}{\lambda Y + \ln(m^2/Q_s^2) + d\sqrt{Y}} \quad (\text{A3})$$

where $\gamma_s = 0.628$ is implied by theoretical arguments [15] and $d = 1.2$ is fixed by fitting to the hadron production data in dA collisions at RHIC. $Y = \ln(1/x)$, with $x = me^{-y}/\sqrt{s}$. The quark dipole scattering amplitude is given by

$$N_F(\mathbf{r}, 0, y) = 1 - \sqrt{1 - N_A(\mathbf{r}, 0, y)} \quad (\text{A4})$$

which follows from (22).

We used the bCGC model [9] with a modification: we treat the nuclei and proton profiles as step-functions; the saturation scales are assumed to scale with A as $Q_s^2 \propto A^{1/3}$. The advantage of this model – besides its compliance with the known analytical approximations to the BK equation [23] – is that its parameters are fitted to the low x DIS data. The explicit form of the scattering amplitude N is given by

$$N_F(\mathbf{r}, 0, y) = \begin{cases} \mathcal{N}_0 \left(\frac{r^2 \mathcal{Q}_s^2}{4} \right)^\gamma, & r \mathcal{Q}_s \leq 2; \\ 1 - \exp[-a \ln^2(br \mathcal{Q}_s)], & r \mathcal{Q}_s \geq 2, \end{cases} \quad (\text{A5})$$

where \mathcal{Q}_s^2 is the the *quark* saturation scale related to the *gluon* saturation scale Q_s^2 – which we have called simply the ‘saturation scale’ throughout the paper – by $\mathcal{Q}_s^2 = (4/9)Q_s^2$. Its functional form is

$$\mathcal{Q}_s^2 = A^{1/3} x_0^\lambda e^{\lambda y} s^{\lambda/2} \text{ GeV}^2, \quad (\text{A6})$$

where s is the square of the center-of-mass energy and y is rapidity with respect to the central rapidity. The anomalous dimension is

$$\gamma = \gamma_s + \frac{1}{c \lambda (\ln \sqrt{s} + y)} \ln \left(\frac{2}{r \mathcal{Q}_s} \right). \quad (\text{A7})$$

Parameters $\gamma_s = 0.628$ and $c = 9.9$ follow from the BFKL dynamics [23], while $\mathcal{N}_0 = 0.7$ and $\lambda = 0.28$ are fitted to the DIS data. Constants a and b are uniquely fixed from by the requirement of continuity of the amplitude and its first derivative.

-
- [1] D. Kharzeev and K. Tuchin, Nucl. Phys. A **770**, 40 (2006) [arXiv:hep-ph/0510358].
 - [2] D. Kharzeev, E. Levin, M. Nardi and K. Tuchin, Nucl. Phys. A **826**, 230 (2009) [arXiv:0809.2933 [hep-ph]].
 - [3] D. Kharzeev, E. Levin, M. Nardi and K. Tuchin, Phys. Rev. Lett. **102**, 152301 (2009) [arXiv:0808.2954 [hep-ph]].
 - [4] L. D. McLerran and R. Venugopalan, Phys. Rev. D **49**, 2233 (1994), Phys. Rev. D **49**, 3352 (1994),
 - [5] Y. V. Kovchegov, Phys. Rev. D **60**, 034008 (1999) [arXiv:hep-ph/9901281].
 - [6] Y. V. Kovchegov, Phys. Rev. D **54** (1996) 5463 [arXiv:hep-ph/9605446].
 - [7] H. Kowalski and D. Teaney, Phys. Rev. D **68**, 114005 (2003) [arXiv:hep-ph/0304189].
 - [8] C. Marquet, R. B. Peschanski and G. Soyez, Phys. Rev. D **76**, 034011 (2007) [arXiv:hep-ph/0702171].
 - [9] H. Kowalski, L. Motyka and G. Watt, Phys. Rev. D **74**, 074016 (2006) [arXiv:hep-ph/0606272].
 - [10] I. Balitsky, Nucl. Phys. B **463**, 99 (1996) [arXiv:hep-ph/9509348];
 - [11] A. H. Mueller, Nucl. Phys. B **335**, 115 (1990).
 - [12] Y. V. Kovchegov, Nucl. Phys. A **692**, 557 (2001) [arXiv:hep-ph/0011252].
 - [13] A. Dumitru, A. Hayashigaki, J. Jalilian-Marian, Nucl. Phys. A **770**, 57-70 (2006). [hep-ph/0512129].
 - [14] D. Kharzeev, Y. V. Kovchegov and K. Tuchin, Phys. Lett. B **599**, 23 (2004) [arXiv:hep-ph/0405045].
 - [15] A. H. Mueller, D. N. Triantafyllopoulos, Nucl. Phys. B **640**, 331-350 (2002). [hep-ph/0205167].
 - [16] S. S. Adler *et al.* [PHENIX Collaboration], Phys. Rev. Lett. **96**, 012304 (2006) [arXiv:nucl-ex/0507032].
 - [17] A. Adare *et al.* [PHENIX Collaboration], Phys. Rev. Lett. **98**, 232301 (2007) [arXiv:nucl-ex/0611020].
 - [18] A. Adare *et al.*, arXiv:1103.6269 [nucl-ex].
 - [19] P. Pillot, f. t. A. Collaboration, [arXiv:1108.3795 [hep-ex]].
 - [20] T. Matsui and H. Satz, Phys. Lett. B **178**, 416 (1986).
 - [21] K. Tuchin, Nucl. Phys. A **798**, 61 (2008) [arXiv:0705.2193 [hep-ph]].
 - [22] K. J. Golec-Biernat and M. Wusthoff, Phys. Rev. D **59** (1998) 014017 [arXiv:hep-ph/9807513], Phys. Rev. D **60** (1999) 114023 [arXiv:hep-ph/9903358].
 - [23] E. Iancu, K. Itakura and L. McLerran, Nucl. Phys. A **708**, 327 (2002) [arXiv:hep-ph/0203137].
 - [24] E.V. Shuryak, Sov. J. Nucl. Phys **28** (1978) 408.
 - [25] D. Kharzeev, H. Satz, Phys. Lett. B **334**, 155-162 (1994). [hep-ph/9405414].